Monthly Notices
of the
ROYAL ASTRONOMICAL SOCIETY

Mon. Not. R. Astron. Soc. **418,** 1127–1137 (2011) doi:10.1111/j.1365-2966.2011.19560.x

Design and development of an optical-fibre-based Integral Field Unit (IFU) on the IUCAA 2-m telescope

Mudit K. Srivastava,[1,2⋆] A. N. Ramaprakash,[1⋆] Hillol K. Das,[1] Mahesh P. Burse,[1] Pravin A. Chordia,[1] Abhay A. Kohok[1] and Chaitanya V. Rajarshi[1]

[1]*Inter University Centre for Astronomy and Astrophysics, Post Bag 4, Ganeshkhind, Pune 411007, India*
[2]*Leibniz-Institut für Astrophysik Potsdam (AIP), An der Sternwarte 16, 14482 Potsdam, Germany*

Accepted 2011 July 31. Received 2011 July 24; in original form 2011 May 17

ABSTRACT

An optical-fibre-based Integral Field Unit (IFU) has been developed for the Inter-University Centre for Astronomy and Astrophysics (IUCAA) Faint Object Spectrometer and Camera (IFOSC), the main back-end instrument on the IUCAA 2-m telescope at Girawali, Pune, India. This IFU enables IFOSC to perform two-dimensional spectroscopy of extended astronomical objects and is being used as one of the modes of IFOSC. Based on the concept of coupling the telescope focal plane with the spectrograph slit using a fibre bundle, the IFU (named the Fibre-based Integral Field Unit for IFOSC, hereafter FIFUI) uses 100 optical fibres, each associated with a tiny lenslet on its tip, to sample the incoming field of view spatially. In addition, FIFUI uses some coupling optics to realize this two-dimensional interface. FIFUI offers three different spatial sampling scales of 0.8, 1.0 and 1.2 arcsec fibre^{-1}. It is optimized for the visible spectrum and for a field of view of $\sim 13 \times 6$ arcsec^2 on the sky for the nominal 1-arcsec sampling mode. FIFUI was commissioned on the IUCAA 2-m telescope during 2010 February–March after a series of sky tests and science-verification observations and a data-analysis pipeline was developed to extract the spectra and reconstruct the sky maps. Here we report on the development of FIFUI, including its opto-mechanical design and commissioning observations.

Key words: instrumentation: spectrographs – techniques: imaging spectroscopy.

1 INTRODUCTION

Integral-field spectroscopy (IFS) is a powerful observing technique that allows the collection of spectra of each spatial element in a two-dimensional (2D) field of view. IFS offers several advantages over the conventional long-slit approach, e.g. minimal slit losses, no need for precise target acquisition, ease in removing the effects of atmospheric dispersion (Arribas et al. 1999), etc. Due to all these advantages, integral-field spectroscopy has opened up many new astronomical research areas, such as the studies of nuclear regions of active galactic nuclei (AGNs), star-formation regions, planetary nebulae, supernova remnants, 2D spectroscopy of various kinds of galaxies, etc.

The instrumentation for IFS has matured significantly over the last two decades and, although various approaches to this technique have been developed, the most common method is to use an integral-field spectrograph. A general integral-field spectrograph consists of two conceptually separate entities that are coupled using a suitable optical interface. The first is a *spatial* unit, called an Integral Field Unit (IFU), which samples the input field of view into the required spatial elements and, after suitably reformatting, feeds light from each of the spatial elements into the second unit. The second unit happens to be a spectrograph that disperses and records the spectra of spatial elements individually, i.e. without any overlap. A number of current and future integral-field spectrographs employ one of the two most popular variants of the IFU, namely (i) optical-fibre-based (e.g. the SPIRAL IFU on the Anglo-Australian Telescope (AAT, Kenworthy, Parry & Taylor 2001), PMAS on the Calar Alto Telescope (Roth et al. 2005), GMOS-IFU on the Gemini-North Telescope (Allington-Smith et al. 2002a)) and (ii) image-slicer based (e.g. AIS-IFU for the Penn State near-IR Imager and Spectrograph (PIRIS, Ren & Ge 2004), GNIRS-IFU on the Gemini-South Telescope (Allington-Smith et al. 2006), MUSE on the Very Large Telescope (VLT, Laurent et al. 2006), MIRI on the *James Webb Space Telescope* (Wright et al. 2008)). Each of the two approaches has associated advantages and disadvantages and these have been discussed in detail in the literature. While most proposed future integral-field spectrographs are still being developed for big (4–10 m class) and giant (25 m or greater) telescopes, the importance of IFS is still significant for smaller telescopes.

⋆E-mail: mudit@iucaa.ernet.in; mudit@aip.de (MKS); anr@iucaa.ernet.in (ANR)

Considering the success of integral-field spectroscopy and IFU-based systems in recent astronomical research, and in view of the interest expressed by many current and upcoming astronomical observatories around the world in acquiring this powerful observing tool, a programme to develop IFU technology in India was initiated at the Inter-University Centre for Astronomy and Astrophysics (IUCAA), Pune, India. Here we report on the design and development of an optical-fibre-based IFU for IUCAA Girawali Observatory (IGO) near Girawali, Pune, India, which houses a modern 2-m $f/10$ telescope. This IFU is being used as a mode of the IUCAA Faint Object Spectrograph and Camera (IFOSC), an instrument mounted on the Cassegrain port of the telescope.

2 DESIGN OF THE IFU ON THE IUCAA TELESCOPE

IGO houses a 2-m, $f/10$ optical and near-infrared telescope (Das et al. 1999). Currently the IUCAA telescope is equipped with an imager-spectrograph named the IUCAA Faint Object Spectrograph & Camera (IFOSC) on its direct Cassegrain port (Gupta et al. 2002). Designed for seeing limited observations, IFOSC uses a 2 K $\times$ 2 K thinned back-illuminated E2V CCD with a pixel size of 13.5 µm. With a spatial sampling scale of 44 µm arcsec^{-1}, this provides an image scale of $\sim$3 pixel arcsec^{-1}. IFOSC is designed to work in the visible regime (3500–8500 Å) with a field of view of 10.5 arcmin on a side. In addition to U, B, V, R and I filters, it also contains several grisms with resolutions from 190–3700. IFOSC is attached to the main Cassegrain port of the telescope through a mechanical interface named the calibration unit (Fig. 1). The calibration unit was designed to provide a buffer between IFOSC and the Cassegrain port of the telescope and it has two filter wheels driven by stepper motors. These wheels carry several narrow-band filters and a fold mirror, which can direct light into IFOSC from a set of lamps for flat-field and spectral calibration. During the observations, these wheels are moved using an automated control system (Srivastava et al. 2009) to bring the desired component (filter or fold mirror) into the path of the telescope beam.

As IFUs in association with a traditional spectrograph offer a preferred way to perform area spectroscopy over a small field of view, the idea of an IFU to be used with IFOSC was thought to be

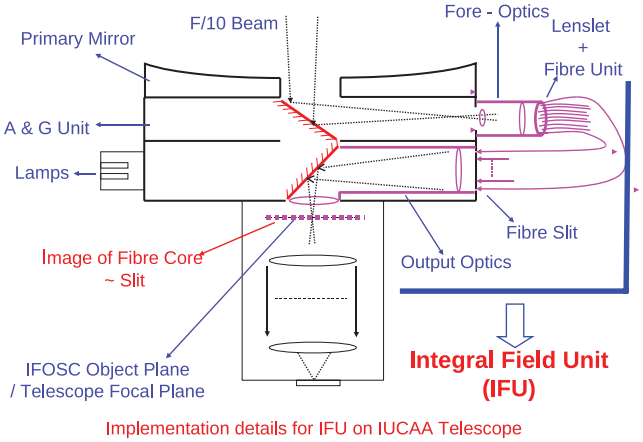

Figure 1. Schematics showing the implementation details for FIFUI as a side-port instrument on the IUCAA telescope. The fore-optics of FIFUI is mounted on a side port of the telescope to accept the telescope beam. The fibre slit is terminated at the wall of the calibration unit and is re-imaged on the IFOSC's slit/object plane by the output optics.

the most convenient approach for 2D spectroscopy on the IUCAA telescope. The *optical fibre plus lenslet* based approach was chosen, as the flexibility of the fibres turned out to be a great advantage given the pre-existing instrumentation set-up on the IUCAA telescope. However, for several reasons discussed below, the design of an IFU on the IUCAA telescope departs from the conventional approaches of IFU development.

2.1 IFU design constraints on the IUCAA telescope

Inserting an IFU between the IUCAA telescope and the IFOSC presented a range of design constraints. The IFU was required to be designed as an observing mode of the IFOSC without affecting its normal modes of operation. Furthermore, in addition to several issues related to fibre-based system design, the fact that the opto-mechanical parameters of IFOSC were matched by design with those of the IUCAA telescope has also put severe constraints on various defining parameters of the IFU. The following factors played a crucial role while designing the IFU.

(i) The IFOSC converts an incoming $f/10$ beam from the telescope to $f/4.5$ (i.e. a demagnification of 2.2) to achieve proper sampling of the recorded images on the CCD. This, when coupled with the dimension of the CCD ($\sim$27 mm), restricts the space available on the IFOSC entrance plane to $\sim$59 mm, thus limiting the size of the one-dimensional (1D) fibre slit and hence the number of fibres in the IFU.

(ii) Due to the existing mechanical configuration of the IFOSC on the telescope, it was not possible to route the fibres through/inside the existing instrumentation set-up and physically to couple the fibre slit directly at the IFOSC entrance. This prevented the use of several conventional means of fibre coupling to the spectrograph, such as using the microlens array at the slit end (Allington-Smith 2006). Therefore, the fibre slit was required to be re-imaged on the IFOSC entrance plane.

(iii) Due to the mechanical interface between the IFOSC and calibration unit (mounting flange etc.), it is not possible to place any optical component between the IFOSC entrance plane and the filter wheel in the calibration unit. As this distance is roughly 80 mm, this demands that the last element of re-imaging optics has to be at least $\sim$80 mm away from the image plane of such optics.

(iv) The space constraints on the telescope and within the calibration unit limit the size and number of components of optical elements to be used to re-image the fibre slit.

(v) The IFU spatial sampling scheme was constrained by the A–Ω relationship for the optical system. Given the telescope plate scale ($\sim$10 arcsec mm^{-1}) and $f/\#$, the A–Ω product for a sampling fibre should be a constant. As the IFOSC will only accept an $f/10$ beam, this puts a lower limit constraint on the projected slit width (and hence the size of the fibre core) and spectral resolution element.

(vi) The focal-ratio degradation (FRD) characteristic of optical fibres was an unknown parameter during the initial phase of design, thus efforts to minimize FRD were given serious consideration.

(vii) The size of the lenslet (used to sample the input image) is a critical parameter in most of the *lenslet plus fibre* based IFUs. A smaller lenslet will always be preferred as it produces fewer aberrations at the pupil, which in turn define the size of the fibre core and hence slit width. However, to allow easy handling and assembling of the lenslets in the laboratory the minimum size of lenslets was restricted to 2 mm.

With the existing limitations of the IFOSC set-up and characteristics discussed above, a couple of trade-offs have been made to

achieve the best possible performance for the IFU. As the telescope images are seeing-limited (∼1 arcsec FWHM), spatial sampling close to seeing scales (*one seeing element per fibre*) has been chosen. Since the number of optical fibres is constrained by a strict space limit, this results in an upper limit on the field of view of the IFU. To allow for the varying seeing conditions at the IGO, provisions for three different spatial sampling scales have also been made for the IFU. As will be discussed in the next section, to enable all these requirements a rather unconventional design and implementation plan has been adopted for the IFU on the IUCAA telescope.

2.2 Concept and implementation of the IFU on IUCAA: fibre-based IFU for IFOSC (FIFUI)

Taking advantage of the availability of the side ports on the IUCAA telescope, the IFU (named the Fibre-based Integral Field Unit for IFOSC, hereafter FIFUI) has been conceptualized as a side-port instrument. The implementation plan of the IFU is shown in Fig. 1. A fold mirror (within the telescope) is used to bring the light out of the side port, which also serves the purpose of blocking the direct view of the telescope beam by IFOSC. Once the telescope beam is taken off the side port, it is fed to the *fore-optics*, which is designed to provide the necessary telecentric magnification to the image, picked from the telescope focal plane. Once magnified, the *lenslet+fibre unit* samples this image through individual lenslets that feed the collected light into the optical fibres. Hexagonal shaped lenslets are used to form a continuous 2D surface and an optical fibre is placed behind each lenslet. Each lenslet produces a small pupil image on the fibre core, avoiding light loss due to the inactive part of the fibres.

The other end of the fibre bundle is arranged in a 1D fibre slit, to be fed to the IFOSC. As direct coupling of this fibre slit to the IFOSC was not possible, a scheme to re-image the fibre slit on to the IFOSC entrance was devised. The slit end of the *lenslet+fibre unit* was terminated at the wall of the calibration unit. Another imaging optics (*output optics*) is designed and integrated within the calibration unit to re-image the fibre slit at the IFOSC entrance. As shown in Fig. 1, the *output optics* contains a mirror to fold the beam into the IFOSC. Mounting this fold mirror on to a filter wheel in the calibration unit and putting it in the beam path will ensure that the fibre slit is re-imaged at the IFOSC entrance. Thus, in this scheme only a couple of mirrors are then required, placed in the path of the input telescope beam and output fibre beam, for the IFOSC to work in IFS mode. For the calibration of IFU spectra, separate spectral calibration lamps are provided in front of the fore-optics, the light from which is folded into the fibre input through the *fore-optics* by another fold mirror.

2.3 Parameters and optical design of the FIFUI

The primary FIFUI parameters include field of view, spatial sampling, number of spatial elements (i.e. number of fibres), spacing of output spectra, spectral resolution, etc. However, not all of these are independent from each other. Although a fast input beam would give better FRD performance (Heacox 1986; Clayton 1989), it would also cause a fast-emerging beam (f/out ∼ f/in) at the fibre output. This would require a higher magnification from the output optics to convert this beam into a $f/10$ beam, and would cause wider pseudo-slit width, lower spectral resolution and space restriction on the 1D physical fibre slit. A design trade-off was made concerning the magnification and performance of the output optics, spectral resolution, physical size of the fibre slit, number of fibres and FRD characteristics of the fibres. This led to the following parameters for optimal performance.

(i) As the FRD performance of fibres from Polymicro Fibres (Polymicro Technologies, Phoenix, AZ) has been reported by Haynes et al. (2004), the same make of fibres was chosen for FIFUI. Considering their FRD characteristic curves as a guideline, it was decided to feed fibres with an $f/4$ beam and to collect an $f/4$ beam at the fibre output. This beam at the output would contains ∼96 per cent of the input light (Haynes et al. 2004). These estimates were reconfirmed during laboratory tests of FRD in these fibres.

(ii) As the IFOSC is designed to accept an $f/10$ or slower beam only, the output optics converts $f/4$ into $f/10$ by providing a magnification of 2.5.

(iii) The maximum possible physical size of the fibre slit could then be $\sim 59/2.5 = 23.6$ mm. Therefore, 100 optical fibres at a pitch of ∼200 μm were accommodated in the fibre slit, thereby fixing the number of spatial elements of the FIFUI. Due to the aberrations in the output optics, 70-μm fibre cores behave equivalent to ∼90 μm when projected as the pseudo-slit. The spacing between the fibres was fixed to be roughly twice the size of the projected fibre cores, to reduce crosstalk and for the ferrules providing mechanical strength to the fibres.

(iv) The centre-to-centre spacing of 200 μm between fibre cores in the slit would translate at the CCD detector as a centre-to-centre separation of ∼17 pixels between spectral traces of two fibres.

(v) At the input end, the fibres are matched with the seeing of the observatory. Along with the nominal sampling scale of 1.0 arcsec fibre^{-1}, two other sampling scales of 0.8 arcsec fibre^{-1} and 1.2 arcsec fibre^{-1} have also been considered. These samplings are attained by the *fore-optics* module, which provides three corresponding magnifications.

(vi) Hexagonal shaped plano-convex lenses of 2.1 mm diameter are used to feed light into the fibre with an $f/4$ beam. Theoretical estimates for the pupil diameter at the fibre entrance are 31, 40 and 47 μm for sky-sampling scales of 0.8, 1.0 and 1.2 arcsec fibre^{-1} respectively. Optical modelling of these lenslets was done using the optical design software ZEMAX-EE. Due to optical aberrations in the lenslets, the pupil sizes turned out to be 52, 64 and 70 μm respectively. Also, considering possible manufacturing errors in lenslet-to-fibre alignments, a slightly oversized fibre core diameter of 70 μm was chosen to match the pupil image, optimizing the system for 1.0-arcsec sampling.

(vii) The minimum width of the projected fibre slit will be $2.5 \times 70 = 175$ μm (∼1.75 arcsec). This is the lower limit of the width of the pseudo-slit. The final shape and size of the pseudo-slit will be dominated by aberrations in the *output optics*.

(viii) The input ends of the fibres are arranged in a way such as to sample a $\sim 13 \times 6$ arcsec^2 field of view for the sampling scale of 1.0 arcsec fibre^{-1}.

The combined effects of aberrations in lenslets, oversized fibre cores and aberrations in output optics lead to widening of the projected slit width at the IFOSC entrance plane. While a 1-arcsec spatial element would correspond to a slit width of 100 μm at the IFOSC entrance plane/telescope focal plane, the projected fibre pseudo-slit width was estimated to be 225 μm (∼2.25 arcsec), thus degrading the spectral resolution by the same factor. With this slit width, the grisms in the IFOSC should then be able to provide resolutions between 8–10 Å over a wavelength range 4500–8500 Å.

The design parameters of the IFU are given in Table 1. The optics for each of the modules (discussed above) was designed using ZEMAX-EE. The designs were optimized for the wavelength range

Table 1. Summary of FIFUI parameters on the IUCAA telescope.

Parameters	Values
Number of fibres	100
Sampling pattern	Hexagonal using lenslets
Sampling scale	1.0, 0.8 and 1.2 arcsec fibre^{-1}
Field size	12.6 × 6.4 arcsec^2 [a]
Fore-optics magnification	20.6, 25.8 and 17.2[b]
Fibre core diameter	70 μm
Slit length	20 mm
Output optics magnification	2.5

[a]With a sampling scale of 1 arcsec fibre^{-1}.
[b]For sampling scales of 1.0, 0.8 and 1.2 arcsec fibre^{-1} respectively.

4500–8500 Å. The fore-optics consists of an achromatic doublet lens (made up of N-FK51 and KF9 glasses from Schott Optical Glasses, SCHOTT AG, Mainz, Germany) and a singlet lens (made up of N-FK51 glass from Schott Optical Glasses). Depending on the mode of sampling, three different achromatic doublet lenses with different focal lengths are used to provide magnification of 20.6 (for 1 arcsec fibre^{-1}), 25.75 (for 0.8 arcsec fibre^{-1}) and 17.17 (for 1.2 arcsec fibre^{-1}), while the same singlet lens is used in all three cases. For a field of view of 20 × 20 arcsec^2 (∼2 mm × 2 mm on the telescope focal plane) the fore-optics provides diffraction-limited performance. The plano-convex lenslets are designed with N-FK51 glass (from Schott Optical Glasses) having a diameter of 2.1 mm. Optical fibres of FBP make from Polymicro Technologies, USA have been used for the IFU. The output optics consists of two singlet lenses (made up of BK7 glass from Sumita Optical Glasses, Saitama City, Japan) and an achromatic doublet lens (made up of PFK85 from Sumita Optical Glasses and KF9 glasses from Schott Optical Glasses). A fold mirror is used to bend the optics by 90° to re-image the fibre slit at the IFOSC entrance. The fold mirror and following plano-convex lens are mounted on two separate wheels inside the calibration unit. These elements are moved in and out to enable/disable the IFU mode of the IFOSC. Fig. 2 is a spot diagram at the detector showing the performance of the output optics with the IFOSC. Due to aberrations in the output optics, the 70-μm core size corresponds to a slit width of ∼2.25 arcsec.

Tolerance analysis of various modules of FIFUI was carried out in consultation with the manufacturers of the optics and mechanical parts. The optical design of each module has undergone a number

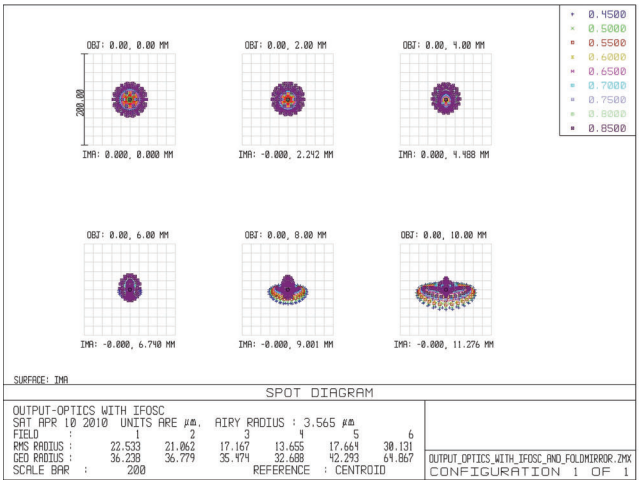

Figure 2. Spot diagram for the output optics with IFOSC at the IFOSC image plane (i.e. at the detector).

of iterations as per manufacturer's suggestions regarding availability of glasses, test plate radii, achievable manufacturing tolerances, cost etc. In the fore-optics design, the achromatic doublets are the most important and critical components of the design. The high magnification and large length of the design put a very tight tolerance of ±5 μm on the centring of the two components of the doublet with respect to each other. The other manufacturing tolerances were industry standard: ±25 μm for the radii of curvatures and ±50 μm for the thickness of the components. The lenslets have tighter tolerances of ±10 μm for both radii of curvature and thickness of the components. In the output optics also, the achromatic doublet was required to have its components centred within ±5 μm, while the tolerances on the radii of curvature and thickness of the components were standard ±50 μm. All the optical components except the glass plate were coated with broad-band anti-reflection coating over the wavelength range 4500–8500 Å with a reflectance of less than 1 per cent. The other specifications (e.g. surface quality λ/4 per inch, power/irregularity 4/1 and scratch/Dig 40/20) were chosen as needed for scientific astronomical imaging applications.

3 FABRICATION AND OPTO-MECHANICAL ASSEMBLY OF FIFUI

The constraints imposed on the optical design of FIFUI also prevail in developing the opto-mechanical environment for the IFU. To achieve the objectives set up by the optical design, it is necessary to have a mechanical environment that would ensure correct distances, alignment, etc. within the specified optical tolerances. This include the design and fabrication of fibre units to hold the fibre bundle and provide the designed pitch between fibres, fabrication of the lenslet array, mechanical assembly of the fore-optics and assembly and alignment of the output optics with IFOSC on the telescope.

3.1 Fibre unit for the IFU

The *Fibre Units Assembly* consists of two mechanical units, namely the *fibre head-mount unit* and *fibre slit unit*, joined by rubber tubing that carries the optical fibres. The job of the Fibre Units Assembly is to provide an efficient configuration of the optical fibre bundle to reformat a 2D field of view at input into a 1D array at output. This demands a high fill factor and a high degree of spatial precision to reduce coupling losses at the input end. The Fibre Units Assembly has been fabricated keeping these objectives in mind. This includes the construction of fibre units and their polishing at both ends.

The optical fibres have core, cladding and buffer diameters of 70, 98 and 125 μm respectively. In addition, an acrylate jacket of 150 μm diameter is also added to the fibres. The fibre head-mount unit carries 100 optical fibres that are arranged in a specific 'closed packed' pattern using quartz ferrules glued together. A closed packed stack of ferrules was constructed inside a rectangular cavity with 13 rows of ferrules with 19/20 fibres in each row. The central 100 fibres in the middle 8 rows contain optical fibres while the rest of the ferrules act as buffer ferrules. Thus the pitch between optical fibres is set by the outer diameter (OD) of ferrules. The fibres run through rubber tubing from the fibre head-mount unit to the fibre slit unit. This unit has a structure similar to the head-mount unit. The fibres are re-arranged here into two parallel staggered slits. Three layers of buffer ferrules have been provided on either side of the fibre slit. The fibres in each of the two slits are kept evenly spaced and parallel to each other using quartz ferrules. A stagger of ∼200 μm, which is given between the two fibre slits, ensures that the projected spectra on the CCD do not overlap. The

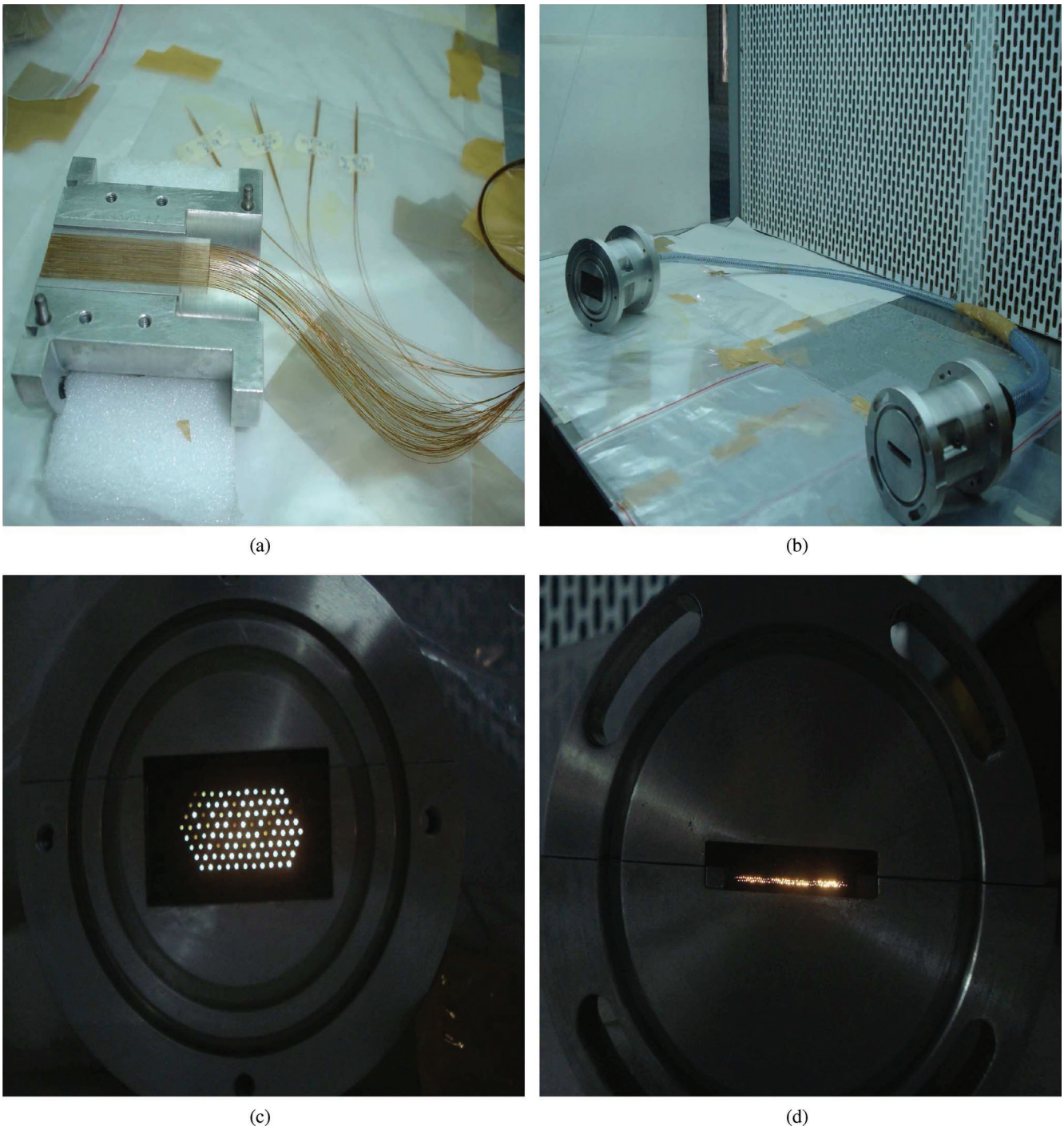

Figure 3. Fabrication of FIFUI fibre units. Panels show various stages in the fabrication of the fibre-unit assembly. (a) Fibre-slit unit in the making. Here fibres are arranged in two parallel slits using quartz ferrules. (b) Fabricated fibre-unit assembly of FIFUI (c) Input end of the assembly: fibre head-mount unit. (d) Output end: fibre slit unit.

fabricated fibre unit assembly is shown in Fig. 3. Finally, both units were polished with aluminum oxide slurry of various particle sizes, i.e. 13.5, 9, 3 and 1 μm, using a fibre-polishing apparatus developed in the instrumentation laboratory.

3.2 Fabrication of the lenslet array

The lenslet array is responsible for sampling of the 2D field of view of the sky. The array has been fabricated with plano-convex hexagonal shaped lenses (lenslets) of 2.1 mm vertex-to-vertex diameter. 100 such lenslets are arranged in the form of a honeycomb structure to provide continuous spatial sampling of the sky image. These 1.5-mm thick lenslets have a radius of curvature of 4.08 mm of the convex surface. For efficient fibre coupling, individual lenslets were required to be aligned with the centre of the fibre core with an accuracy of ±5 μm. A 10.8-mm thick glass window (of S-FPL51 glass, from Ohara Glasses, Kanagawa, Japan) is used as a buffer between the fibre tips and the lenslets. The array has been fabricated over

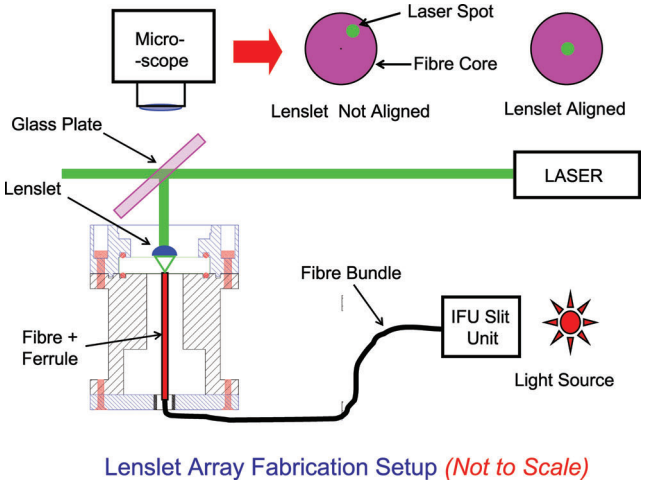

Figure 4. Schematics of the fabrication set-up for the lenslet array fabrication. The fibre cores at the front end of the fibre unit are back-illuminated and monitored through a microscope. A laser beam is adjusted so that it falls perpendicular to the front surface of the illuminated fibre cores. The lenslets (with optical cement applied on the back surface) are then aligned and glued on to the surface of the glass plate, so that the focused laser spot coincides with the centre of the fibre core.

this glass surface, while pressing the glass window on the top of the input fibre unit by another mechanical unit.

A fabrication set-up was developed in the instrumentation laboratory at IUCAA for this purpose. Schematics of this set-up are shown in Fig. 4. The glass window was fixed on the top face of the fibre head-mount unit using a mechanical interface. This whole assembly was mounted on a pair of travelling stages and could be moved in X–Y directions with an accuracy of $\sim$2 μm. A laser beam was then aligned to fall perpendicular to the surface of the glass plate. The fibres in the head-mount unit were back-illuminated to inspect individual fibre cores using a microscope. The head-mount unit was moved using the translational stage so as to obtain a fibre centred with respect to the laser spot. A thin layer of UV-curing optical cement (Norland-61) was then applied to the plane surface of a lenslet and it was placed on the glass window in the path of the laser beam. The lenslet then focused the laser beam on to the tip of the fibre core. The location of the focused laser spot on the fibre core was monitored through the microscope. The position and orientation of the lenslet were then adjusted to centre the laser spot on the fibre core tip. The system was then exposed to UV light for curing without disturbing the lenslet position for $\sim$15 min. Once the lenslet array was fabricated (Fig. 5), the singlet lens of the fore-optics was mounted on the fibre head unit and secured with a retainer ring.

3.3 Opto-mechanical assembly of FIFUI

The mechanical layout of FIFUI is divided into two parts, namely the *front unit* and the *output-optics mechanical assembly*. The front unit is the the mechanical interface between FIFUI and the telescope. It is mounted on one of the side ports of the telescope to provide mechanical support for the fore-optics section of FIFUI. It contains the three achromatic doublet lenses of the fore-optics. A combination of one achromatic doublet with the singlet lens is used to provide one sampling mode. The achromatic doublets are mounted on a one-dimensional *linear motorized translation stage* (from Newport Corporation, Irvine, CA), therefore any one of the three sampling scales can be achieved by moving the corresponding

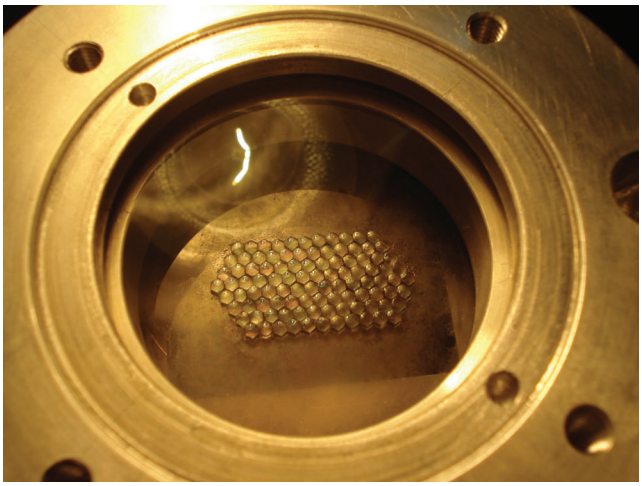

Figure 5. The fabricated lenslet array.

achromatic doublet into the path of the light beam. A fold mirror is also attached to the optical design, considering that the space available outside the side port is not enough for a linear design. Provision for calibration lamps is also made for this unit, for wavelength calibration of the observed spectra. Light from these lamps is fed to the fore-optics section of FIFUI using a pneumatically actuated second fold mirror which also blocks the light from the telescope. The front unit has been designed and developed using off-the-shelf space frame components from LINOS Photonics, Munich, Germany.

The output-optics mechanical assembly is the mechanical interface that integrates the output optics within the existing calibration unit on the telescope. The calibration unit contains two wheels that are driven by stepper motors. A schematic of the output-optics mechanical assembly is shown in Fig. 6. The output-optics assembly consists of three parts.

(1) Main body, which contains the first two lenses of the output optics. The fibre slit unit is coupled to the output optics through this part. It is mounted on the wall of the calibration unit.

(2) The fold-mirror mount is a mechanical assembly to fix a fold mirror at 45°. It is mounted on one of the two filter wheels inside the calibration unit.

(3) Lens mount, to hold the third lens of the output optics. It is fixed to the other filter wheel inside the calibration unit. The output optics is aligned with the IFOSC's optic axis.

The mechanical design layouts of these parts were prepared using the AUTOCAD software and different mechanical components were fabricated by local manufacturers. Finally these two parts were joined together by the fibre-unit assembly by ensuring the correct orientation of the fibre slit on the IFOSC CCD. Fig. 7 shows the final FIFUI arrangement mounted on the telescope.

4 FIFUI COMMISSIONING TESTS ON THE IUCAA TELESCOPE

As FIFUI was developed to be part of a pre-existing set-up, the commissioning tests for FIFUI not only allowed characterization of the instrument but also were essential to plan the strategy for integral-field observations with the IUCAA telescope. These commissioning tests involved several complex issues like fibre-to-fibre mapping from input to output, determination of the FIFUI footprint on the CCD, determination of focus positions for IFS observations, pointing issues, throughput estimation, etc.

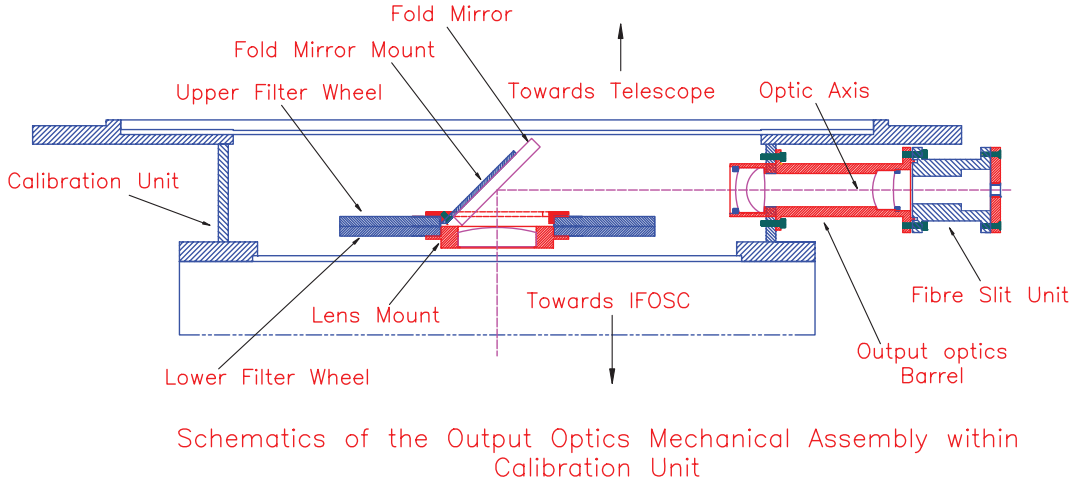

Figure 6. Schematics of the output optics mechanical assembly.

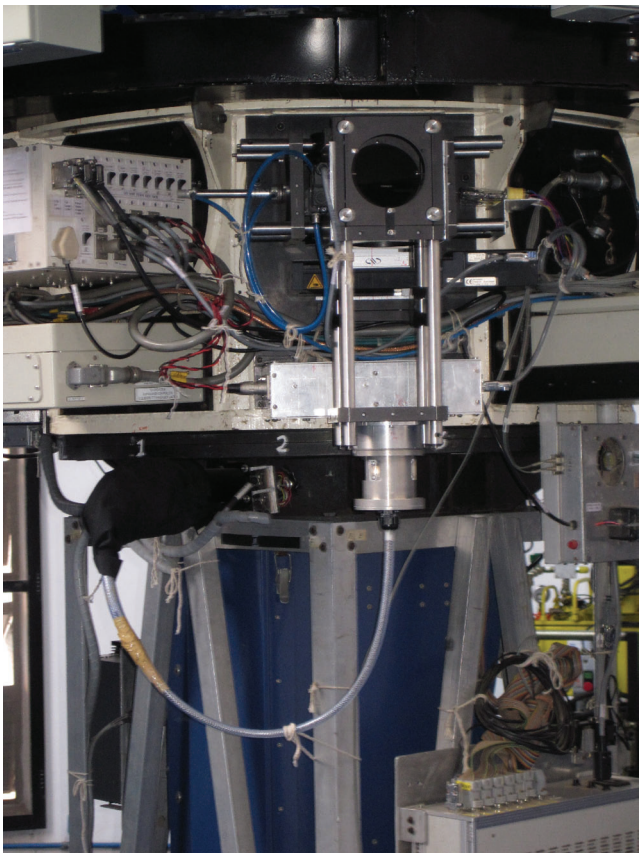

Figure 7. FIFUI installed on the telescope side port. FIFUI's front mechanical unit is shown, along with fibre units. The front mechanical unit provides a mechanical interface between the fore optics and the telescope. The fore-optics components are housed within and it also consists of calibration lamps for FIFUI's calibration.

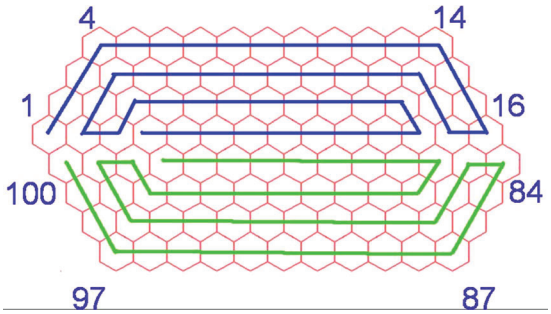

Figure 8. Arrangements of the fibres (with hexagonal lenslets) at the input end of FIFUI. The blue and green lines show the numbering scheme used for lenslet-to-slit mapping. The leftmost fibre in the upper half is numbered 1 and the blue curve follows the path with an increasing index number of lenslets until its reaches number 50 in the centre of the array. Similarly, the green curve starts with index 100 from the leftmost lenslet in the lower section and traces the lenslets in a spiral way until it reaches index 51 in the centre of the array.

4.1 Lenslet mapping and intensity profile of the fibre slit

Although a one-to-one mapping scheme of the fibres was devised to map fibres from input end to output end, some of the fibres were displaced from their nominal positions during fabrication of the slit. Because of this, neighbouring fibres on the slit do not necessarily fall adjacent on the sky. Thus the arrangements of the fibres in the slit turned out to be quasi-random in nature. The arrangements of the fibres at the input end are shown in Fig. 8 and the corresponding positions of the fibres in the slit in Fig. 9.

During the polishing process, a temporary malfunction of the apparatus caused a few sudden jerks of the polishing disc. These jerks chipped off a few ferrules containing fibres at the output slit unit. This resulted in all together eight cracked or inactive fibres. Given the limitation on available time, it was not possible to continue polishing until the cracks at the fibre tips were removed. Thus, after polishing, the number of active fibres in the IFU turned out to be 92. The fibre pseudo-slit in Fig. 9 shows the combined effects of aberrations and throughput variation on the shape and size of projected fibre cores.

As the imaging performance of the output optics is aberration-dominated, the projected intensity profiles of fibre cores (the pseudo slit) vary as a function of position along the fibre slit. However, the location of the physical fibre slit was not designed to obtain the sharpest image at the centre on the IFOSC entrance plane. Rather it was optimized to a value such that the projected width of the fibre pseudo-slit (for all the fibres) would remain around 2.3 arcsec. In this way, better performance at the edges of the fibre slit was obtained at the cost of slight degradation in the centre of the slit. The nearly uniform full widths at half-maximum (FWHMs) of the

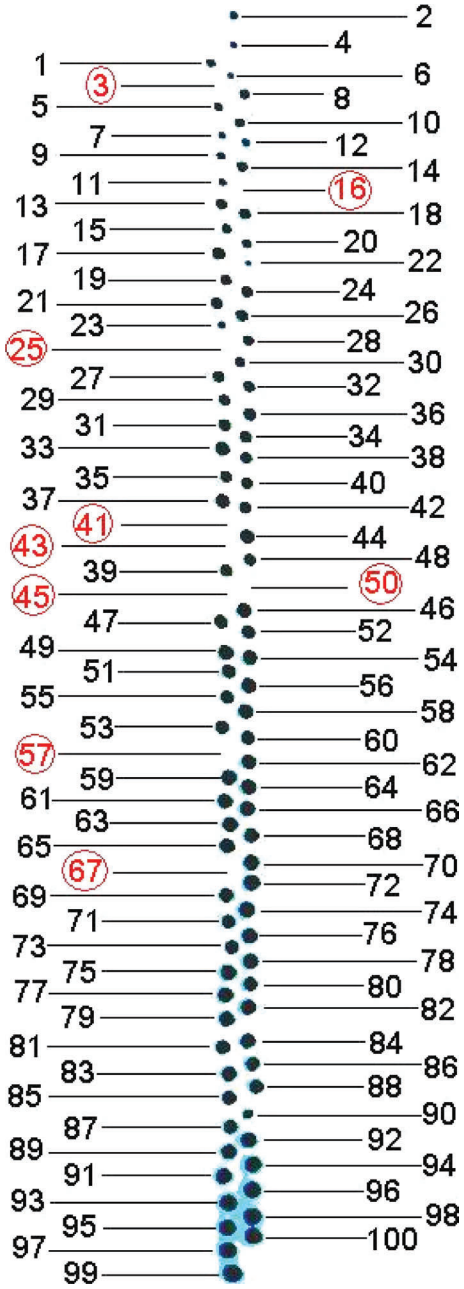

Figure 9. Fabricated FIFUI double slit in reverse contrast, back-illuminated so that the fibre cores are visible. The numbers show the corresponding positions of the fibres on the sky (Fig. 8). It is noted that eight fibres out of 100 are completely broken (shown by red circles). Fibre no. 25 is partially broken and gives a faint output while in use with the calibration lamps.

re-imaged fibre cores are due to proper adjustment of the distance between the fibre slit and the first lens of the output optics, which was achieved as part of the commissioning exercise.

Flat-field sky images of the fibre slit were used to determine the profiles of the re-imaged fibre cores on the detector. Fig. 10 shows the intensity profiles of the re-imaged fibre cores in the dispersion direction. The FWHMs of these profile are found to be in the range ∼4–6 pixels along the slit. Given the image scale of ∼3 pixels arcsec^{-1}, this results in a maximum slit width of <2.3 arcsec (∼7 pixels) for the fibres that are worst affected by the aberrations.

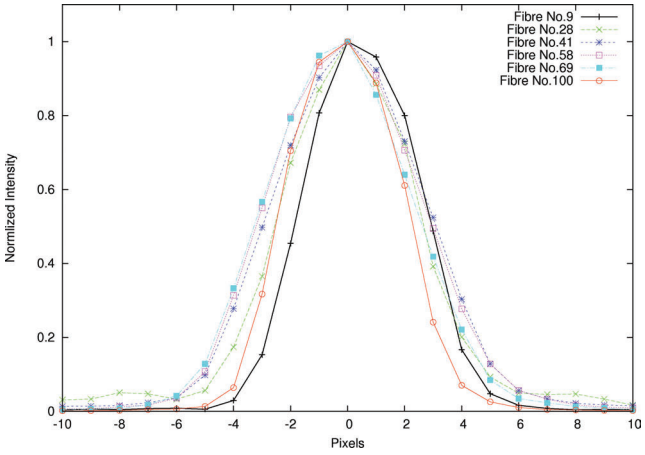

Figure 10. Intensity profiles of some of the projected fibre cores on the detectors. Profiles of six fibre cores along the slit are shown for comparison. These fibre cores are selected along the slit and they illustrate the range of fibre-core profiles seen in the pseudo slit.

4.2 FIFUI on-sky commissioning tests

The performance of FIFUI is highly coupled to the functioning of the telescope and IFOSC. Few parameters of the set-up are required to obtain a target within FIFUI's field of view and to focus it properly. In addition, fibre-to-fibre response variation is also required to be known to calibrate the spectra relatively. Several sky tests were conducted to determine the parameters required to observe with FIFUI, as described below.

(i) The FIFUI field of view has been calibrated with respect to IFOSC's field of view in direct imaging mode. This has been done by mapping individual fibre cores to the pixels of the IFOSC CCD. A point source (star) is observed through a single input fibre to determine this. The reconstructed FIFUI footprints on the IFOSC CCD are shown in Fig. 11 for a sampling scale of 1 arcsec fibre^{-1}. Similar footprints were determined for the other sampling scale.

(ii) To focus the object on the lenslet array surface, relative focus offsets are applied to the position of the secondary mirror of the telescope with respect to its position for IFOSC direct imaging mode. The secondary mirror offset values for sampling scales of 1.0, 1.2 and 0.8 arcsec fibre^{-1} were found to be +0.66, +1.48 and +0.87 mm respectively. These offset values have been found to be consistent over the period 2009 November–2010 February.

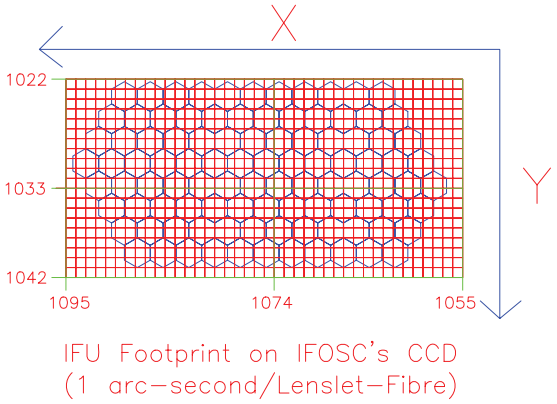

Figure 11. FIFUI footprint on the IFOSC's CCD for a spatial sampling of 1.0 arcsec fibre^{-1}. The lenslets are mapped on corresponding pixels of the CCD as per the sky coordinates.

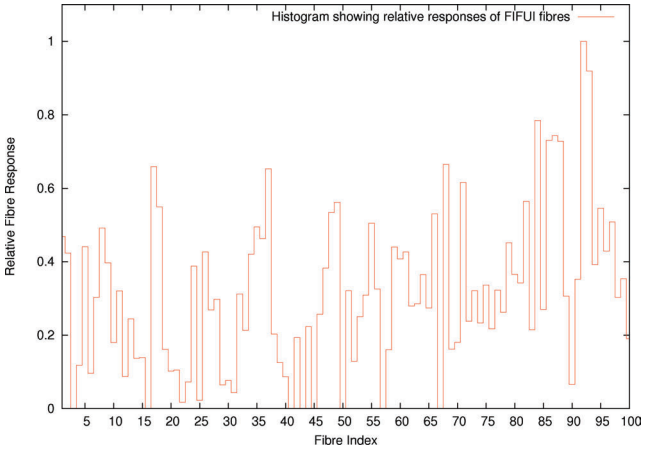

Figure 12. Histogram showing the flat-field response of FIFUI's fibres.

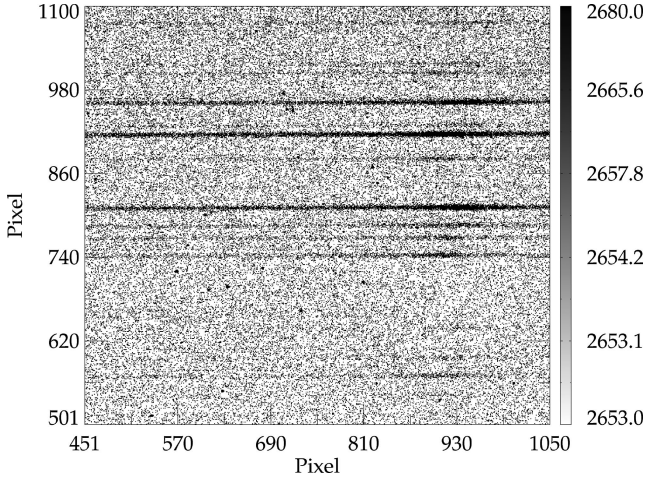

Figure 13. Spectra of the ULIRG Mrk 231 taken through FIFUI, for a 45-min exposure.

(iii) The relative pointing offsets between the three sampling schemes were calculated by determining the positions of a point source (a star) on the IFU input (i.e. on the surface of the lenslet array) and the respective positions on the IFOSC. The translation stage with the fore-optics first lens has also been calibrated as per these offsets.

(iv) The relative response of FIFUI fibres was determined using a series of flat-field observations. Fibre-to-fibre response variation is shown in Fig. 12. The fibre responses were normalized with respect to the maximum-intensity fibre. These relative fibre responses were found to be stable over the period 2009 November–2010 February. It is evident that the flat-field response of the fibres is not uniform compared with other IFUs (Allington-Smith et al. 2002b). This is caused by a systematic variation in the throughput along the fibre slit, produced during the fibre-polishing process. Fibres at one end of the slit show better throughput. This characteristic of the fibre slit is also present in Fig. 9, where high-throughput fibres are seen at the lower end of the slit.

The commissioning observations played a very critical role in defining the strategy for integral-field observations with the IUCAA telescope. Further, they provided several required inputs, as discussed above, for the development of spectral flat-fielding, wavelength calibration, spectral extraction strategies and FIFUI data-cube generation.

5 OBSERVING WITH FIFUI: THE DATA REDUCTION PIPELINE

Observations with the FIFUI require a certain sequence to be followed that ensures proper focus and acquisition of the object within the FIFUI field of view as well as acquisition of other necessary data (calibration, flats, sky, etc.). As mentioned earlier, due to broken or low-throughput fibres there are gaps in the IFS observations of the 2D field being observed. However, these gaps could be could be filled by observing the same field twice with suitable pointing offsets in the repeated observations. The data reduction for FIFUI offers some additional challenges given its complex optical design, two parallel pseudo-slits and pseudo-random mapping of the fibres. Therefore, a basic data-reduction pipeline has been developed particularly to process FIFUI raw data frames to extract individual spectra from the fibres.

The wavelength coverage and resolution of FIFUI spectra are determined by grisms within the IFOSC. Within the IFOSC, IFORS1 (3300–5540 Å), IFOSC7 (3800–6840 Å) and IFOSC8 (5800–8350 Å) grisms cover the visible wavelength regime and, when used with FIFUI, they provide a spectral resolution of 8–10 Å. For our science-verification programme, an ultraluminous infrared galaxy (ULIRG), Markarian 231 (Mrk 231), was selected due to its brightness and compatible angular dimensions with the FIFUI field of view. At a redshift of 0.042, it is one of the best-studied galaxies (Hamilton & Keel 1987) and among the most luminous in the IRAS sample with $L_{\rm IR} \sim 10^{12.04}\,{\rm L}_{\odot}$. The IFOSC8 (5800–8300 Å) grism was used to trace Hα emission. Several observations of ∼30–45 min exposure were taken. Predetermined pointing offsets were given between successive observations to fill the gaps in FIFUI input due to inactive fibres. Calibrations and continuous halogen spectra were taken just before and after the science observations for data-reduction purposes. A section of CCD data frames with FIFUI spectra of Mrk 231 (for a 45-min exposure) is shown in Fig. 13.

FIFUI data reduction, in general, is a complex process. Several general fibre-based IFU data-reduction software packages (e.g. p3d, Sandin et al. 2010; R3D, Sánchez 2006) and instrument-specific reduction algorithms (Zanichelli et al. 2005; Turner et al. 2006; Sharp & Birchall 2010) have been described in the literature, however data reduction for FIFUI offers some unique challenges compared with several existing integral-field spectrographs on other telescopes. As all the fibres in the pseudo-slit are not along a single column and the re-imaged fibre cores in the pseudo-slit are not identical due to aberrations, these two issues puts additional constraints on wavelength calibration of the spectra and are handled with extreme care while reducing FIFUI data. The data-reduction pipeline for FIFUI is developed in C and uses the CFITSIO[1] library routines to manipulate data frames generated in FITS[2] image format.

The basic functions of the routines in the pipeline includes preprocessing of the raw data, determining the position of the spectra on the image frames, profile determination of the fibre spectra, extraction of each individual spectrum, wavelength calibration, fibre-to-fibre response correction and reconstruction of the sky map at any given waveband. All FIFUI raw data are to be pre-processed for bias subtraction and flat-field correction. Science and calibration-lamp spectra are reduced by determining the intensity profiles of the

[1] http://heasarc.nasa.gov/fitsio/fitsio.html
[2] Flexible Image Transport System (FITS).

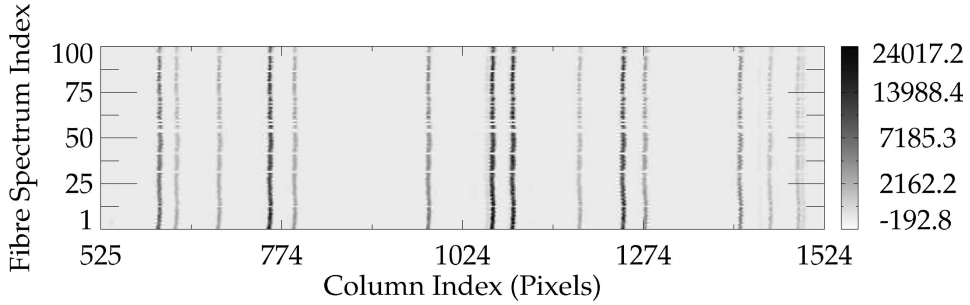

Figure 14. A 2D map for the reduced FIFUI spectra of He–Ne calibration lamps. Columns of this map (*X* axis) correspond to pixels in the dispersion direction and rows (*Y* axis) represent the fibre index. Values of the map are counts of the fibre spectra for a given column pixel. Only the central 1000 columns are shown. The black horizontal strips represent rows corresponding to inactive fibres, where values are kept at zero.

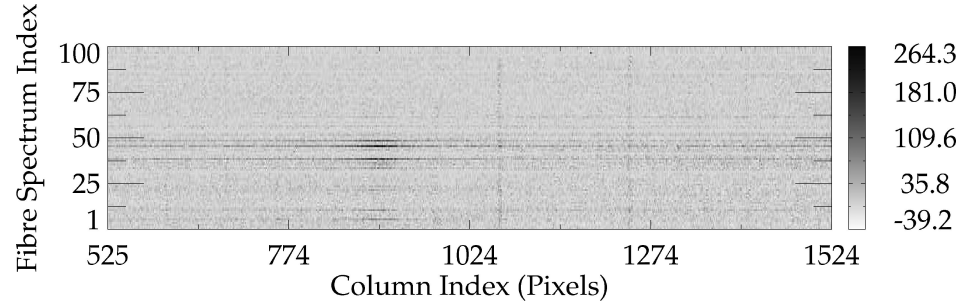

Figure 15. A 2D map for the reduced FIFUI spectra of ULIRG Mrk 231. Other details are the same as for Fig. 14. The presence of sky emission lines can be noted in all fibre spectra.

dispersed fibre spectra in the cross-dispersion direction. The continuous halogen-lamp FIFUI spectra are used to trace the fibre spectra along each of the columns of pre-processed data frames and then in determining the cross-dispersion profiles of the spectra. These cross-dispersion profiles are approximated by Gaussian functions. Thus various profile parameters (like centre, width of the Gaussian, background intensity, etc.) are determined. These parameters are then applied over the science and calibration-lamp FIFUI data to extract individual spectra. Reduced FIFUI spectra of calibration lamps and science data are presented in the form of a 2D map, shown in Figs 14 and 15.

The emission lines in the reduced calibration-lamp data are identified and then used to calibrate the science data. The data-reduction pipeline has been successfully applied to reduce FIFUI spectra of the Mrk 231 ULIRG. A wavelength-calibrated spectrum of Mrk 231 through an FIFUI fibre is shown in Fig. 16 for a 45-min exposure time. A signal-to-noise ratio (SNR) of 14 has been achieved for a single FIFUI fibre in 45 min of exposure time, for a wavelength bin of $\sim$1.2 Å.

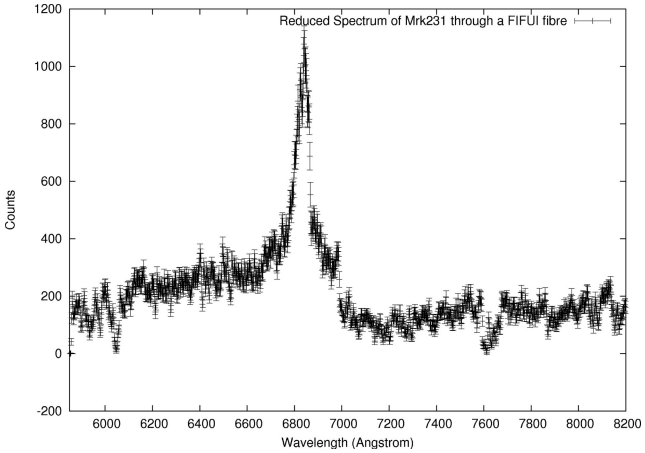

Figure 16. Wavelength-calibrated spectrum of the ULIRG Mrk 231 through a FIFUI fibre. The error bars on the count values are also shown.

6 SUMMARY

Integral-field spectroscopy (IFS) has revolutionized modern astronomical research, with all major observatories now either having or constructing suitable instruments. Considering the significance of this powerful technique in the near future of astronomical research, a programme to develop IFU technology in India was initiated at the Inter-University Centre for Astronomy and Astrophysics (IUCAA), Pune, India. This led towards the development of a fibre-fed integral field unit to be used as a mode of the traditional spectrograph (IFOSC) on the IUCAA 2-m telescope. The IFU was conceptualized as an interface to connect the focal plane of the telescope with the spectrograph slit using a fibre bundle along with several coupling optics. This fibre-based IFU for IFOSC (FIFUI) has been optimized for visible spectra and consists of 100 fibres. The field of view of FIFUI is $\sim$13 arcsec $\times$ 6 arcsec with three modes of sky sampling, i.e 1.0, 0.8 and 1.2 arcsec fibre^{-1}. The projected fibre slit width at the IFOSC entrance is determined to be 2.3 arcsec and, with existing grisms within the IFOSC, FIFUI provides a spectral resolution of $\sim$8–10 Å.

Though FIFUI has been commissioned and used for scientific observations, there still exists the scope to enhance the performance of FIFUI through various improvements, both at hardware and software levels. Though the issue of broken/inactive fibres in FIFUI's field of view has been tackled through an observing strategy and at pipeline level, nevertheless it is desirable to have a fibre unit with all fibres functioning properly. Thus a new fibre unit (along with a

lenslet array) is proposed for development. The FIFUI structure for the IUCAA telescope makes it extremely convenient to replace the old fibre unit with a new one, with no extra effort. A better polishing procedure would also improve the throughput variation of the fibres. There are also issues to be improved in the software domain. Currently, FIFUI is being operated through the direct engineering interface of the instrumentation control software. However, for the common user, a graphical interface (GUI) for FIFUI is required. The FIFUI data-reduction pipeline performs all the basic processing of FIFUI raw data. Still, the options for flux calibration, differential atmospheric refraction correction and sky determination have yet to be incorporated. A GUI for the FIFUI pipeline could also be developed. With all these improvements, the performance of FIFUI could be further enhanced if it were used with a purpose-built spectrograph, thus eliminating the use of output optics and aberrations therein.

FIFUI has been commissioned on the IUCAA 2-m telescope during 2010 February–March. The concept of integral-field spectroscopy through FIFUI has been demonstrated successfully for the first time in India. Various techniques required for the realization of fibre-based IFUs have been developed. These techniques will have wide application in future IFS instrumentation for several upcoming astronomical facilities, not only in India but also around the world.

ACKNOWLEDGMENTS

We are thankful to the members of the Instrumentation Laboratory at IUCAA and IGO support staff for their help and support during the development of FIFUI. We also thank the referee for useful comments and suggestions. MKS thanks the Council for Scientific and Industrial Research (CSIR), India, for the research grant award NO.9/545(25)/2005-EMR-I.

REFERENCES

Allington-Smith J., 2006, New Astron. Rev., 50, 244
Allington-Smith J. et al., 2002a, PASP, 114, 892
Allington-Smith J., Murray G., Content R., Dodsworth G., Miller B. W., Turner J., Jorgensen I., Hook I., 2002b, Exp. Astron., 13, 1
Allington-Smith J. R., Content R., Dubbeldam C. M., Robertson D. J., Preuss W., 2006, MNRAS, 371, 380
Arribas S., Mediavilla E., Garca-Lorenzo B., del Burgo C., Fuensalida J. J., 1999, A&AS, 136, 189
Clayton C. A., 1989, A&A, 213, 5023
Das H. K., Menon S. M., Pranjpye A., Tandon S. N., 1999, Bull. Astron. Soc. India, 27, 609
Gupta R., Burse M., Das H. K., Kohok A., Ramaprakash A. N., Engineer S., Tandon S. N., 2002, Bull. Astron. Soc. India, 30, 785
Hamilton D., Keel W. C., 1987, ApJ, 321, 211
Haynes R., Bland-Hawthorn J., Large M. C., Klein K., Nelson G. W., 2004, Proc. SPIE, 5494, 586
Heacox W. D., 1986, AJ, 92, 2195
Kenworthy M. A., Parry I. R., Taylor K., 2001, PASP, 113, 215
Laurent F., Henault F., Renault E., Bacon R., Dubois J., 2006, PASP, 118, 1564
Ren D., Ge J., 2004, PASP, 116, 463
Roth M. M. et al., 2005, PASP, 117, 620
Sánchez S. F., 2006, Astron. Nachr., 327, 850
Sandin C., Becker T., Roth M. M., Gerssen J., Monreal Ibero A., Böhm P., Weilbacher P., 2010, A&A, 515, 35
Sharp R., Birchall M. N., 2010, Publ. Astron. Soc. Aust., 27, 91
Srivastava M. K., Prabhudesai S. M., Tandon S. N., 2009, PASP, 121, 1112
Turner J. E. H., Miller B. W., Beck T. L., Song I., Cooke A. J., Seaman R. L., Valdés F. G., 2006, New Astron. Rev., 49, 655
Wright G. S. et al., 2008, in Oschmann J. M., Jr, de Graauw M. W. M., MacEwen H. A., eds, Proc. SPIE, Vol. 7010, Space Telescopes and Instrumentation 2008: Optical, Infrared, and Millimeter, 70100T
Zanichelli A. et al., 2005, PASP, 117, 1271

This paper has been typeset from a TEX/LATEX file prepared by the author.